*Acta Cryst.* (1999). B**55**, 203–208

# Conformational behaviour of bridging diphenylphosphido ligands†

John J. Barker and A. Guy Orpen*

*School of Chemistry, University of Bristol, Bristol BS8 1TS, England. E-mail: guy.orpen@bristol.ac.uk*

(*Received 3 September 1998; accepted 29 October 1998*)

## Abstract

Data retrieved from the Cambridge Structural Database for crystal structures containing ($\mu$-diphenylphosphido) metal complexes, $[M_2\{\mu\text{-}PPh_2\}]$ (where $M$ is a $d$-block element), have been analysed to evaluate the conformational behaviour of these species. The observed distribution of torsion angles about the P—C bonds has been compared with the potential energy surface (PES) for phenyl rotations in a representative species $[(AuBr)_2\{\mu\text{-}PPh_2\}]^-$ computed using the universal force field. Good agreement was obtained between the low-energy (<8 kJ mol$^{-1}$ above the global minimum) regions of the PES and the occupied regions of the two-dimensional P—Ph rotor conformation space. Phenyl ring rotations occur by coupled, geared disrotatory and uncoupled conrotatory motions of the phenyl groups in this and other classes of $PPh_2$ rotors.

## 1. Introduction

Bridging phosphido ligands have been widely used in transition metal chemistry in order to provide stability to di- and polymetallic arrays (see, for example, Baker *et al.*, 1990, and references therein). The most common ligand of this type is diphenylphosphide, the conformational behaviour of which is the subject of this paper. The $[M_2\{\mu\text{-}PPh_2\}]$ (where $M$ is a $d$-block element) fragment is a member of a wider family in which a tetrahedral or trigonal centre, $E$, carries two or more aryl substituents. This family includes, of course, all $PPh_3$ complexes (Bye *et al.*, 1982), as well as the organic archetype diphenylmethane, $CH_2Ph_2$ (Dunitz, 1979), and a wide range of $EAr_2$ and $EAr_3$ species ($E$ = B, C, N, O or S; see, for example, Mislow, 1976; Rappoport *et al.*, 1990; Klebe, 1994; Rappoport & Biali, 1997). Although some notable studies of more complex systems containing $PPh_2$ moieties have been reported, including several on triphenylphosphine species (Bye *et al.*, 1982; Norskov-Lauritsen & Bürgi, 1985; Garner & Orpen, 1993) and chelating bis(diphenylphosphino)alkanes (Morton & Orpen, 1992; Hunger *et al.*, 1998), there has been no study reported on the conformational behaviour of this, the simplest diphenylphosphorus member of this family of diaryl rotor systems. The approach taken in this work is twofold: firstly, we have studied the conformations of $[M_2\{\mu\text{-}PPh_2\}]$ species in crystal structures in the Cambridge Structural Database (CSD; Allen & Kennard, 1993) and, secondly, for comparison, the potential energy of a representative species $[(AuBr)_2\{\mu\text{-}PPh_2\}]^-$ has been evaluated using molecular mechanics methods. The methods used allow a semi-quantitative test of the modelling procedures by comparison with a range of structures (Klebe, 1994) rather than the more conventional approach whereby molecular geometries in individual crystal structures are compared with (gas phase) optimized computational models.

## 2. Experimental

### 2.1. *Data retrieval and analysis*

Crystal structures containing the molecular fragment $[M_2\{\mu\text{-}PPh_2\}]$ (where $M$ is a $d$-block metal, *i.e.* Sc–Zn, Y–Cd, La–Hg) were retrieved from the CSD using the *QUEST* program (Allen & Kennard, 1993). The crystallographic data retrieved were screened manually and automatically and only structures which fulfilled all of the following criteria were retained for further analysis: (i) crystallographic $R \leq 0.07$; (ii) mean standard deviation of the C—C bond lengths $\leq 0.03$ Å; (iii) no disorder in the fragment under study; (iv) no unresolved errors in the stored structure; (v) the chemical and crystallographic connectivity matched exactly. A total of 414 $[M_2\{\mu\text{-}PPh_2\}]$ fragments were retrieved from 280 different crystal structures. The orientation of the phenyl rings was described by combining the two C(*ipso*)—P—C(*ipso*)—C(*ortho*) torsion angles for each ring, $\omega_1$ and $\omega_2$, $\omega_3$ and $\omega_4$, as in (1) and (2) below, to give a single torsion for each ring, $\omega_A$ and $\omega_B$, lying in the range 0 to 180° (Dunitz, 1979; Bye *et al.*, 1982);

$$\omega_A = (\omega_1 + \omega_2 + 180)/2, \quad (1)$$

$$\omega_B = (\omega_3 + \omega_4 + 180)/2. \quad (2)$$

The $C_{2v}$ frame symmetry of the $[M_2\{\mu\text{-}PPh_2\}]$ unit and the 180° periodicity of the $\omega$ torsions leads to the torsion-angle permutations listed in Table 1 (Dunitz, 1979) which fill four unit cells of conformation space, spanning the region from −180 to +180° for $\omega_A$ and $\omega_B$.

† Structural systematics part 7. For part 6 see Martín & Orpen [*J. Am. Chem. Soc.* (1996), **118**, 1464–1470].

This 16-fold permutation yields a total of 6624 points in the ($\omega_A$, $\omega_B$) scatter plot (see below).

### 2.2. *Molecular mechanics*

The universal force field (UFF; Rappé *et al.*, 1992) was employed as implemented in the *CERIUS* modelling package (Molecular Simulations Inc., 1994). All calculations were performed on a Silicon Graphics RS 4000 Indigo workstation. A bond-order correction of 1.5 to $M-$P bonds in tertiary phosphines was applied. The force-field atom type for the phosphorus was taken to be P_3_q, the atom type specifically designed for metal complexes. Initial trials on model systems were found to give reasonable agreement with the CSD-derived results noted below. However, the P—C(*ipso*) bond lengths were found to be underestimated by approximately 0.03 Å and the natural bond length of 1.800 Å in the force field was replaced with one of 1.828 Å. No other changes were made. All calculations were carried out without partial atomic charges. The gold centres were taken as force-field atom type Au4+3, a square-planar +3 oxidation state gold atom, this being the closest force-field type to the linear $Au^I$ of the model complex studied, $[(AuBr)_2\{\mu\text{-}PPh_2\}]^-$.

A grid search was used to probe the two-dimensional conformation space. Torsion angles were constrained with a force constant of 4186 kJ mol$^{-1}$ $^{\circ-1}$ to a grid of values selected to include all the unique conformations of the structure. From each point on the grid the structure was optimized to an r.m.s. force of <0.0084 kJ mol$^{-1}$ Å$^{-1}$ using a conjugate gradient algorithm. The crystal structure of the $[N^nBu_4]^+$ salt of $[(AuBr)_2\{\mu\text{-}PPh_2\}]^-$ (Pritchard *et al.*, 1987) was used as a starting geometry and the torsion angles were driven to the required grid points. The torsion angles used were defined as in the CSD study and grid points chosen at

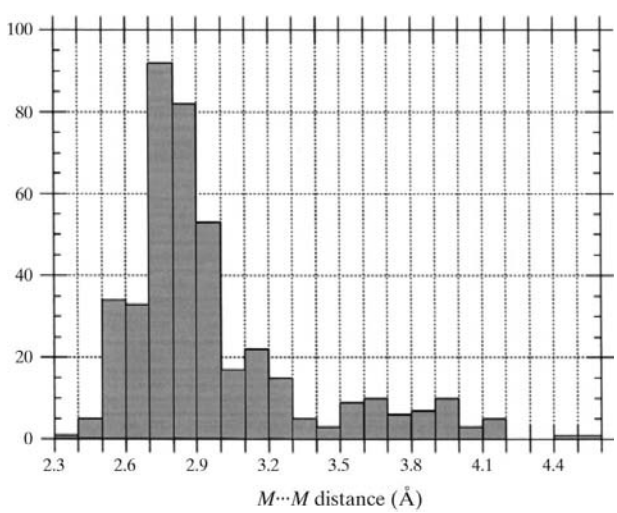


Fig. 1. Histogram of $M\cdots M$ distances (Å) in the structures used in the CSD studies of $[M_2\{\mu\text{-}PPh_2\}]$.

Table 1. *Symmetry permutations applied to conformations for* $[M_2\{\mu\text{-}PPh_2\}]$ *and* $[(AuBr)_2\{\mu\text{-}PPh_2\}]^-$

| | | |
|---|---|---|
| $E$ | $\omega_A$ | $\omega_B$ |
| | $\omega_A - 180$ | $\omega_B$ |
| | $\omega_A$ | $\omega_B - 180$ |
| | $\omega_A - 180$ | $\omega_B - 180$ |
| $C_2$ | $\omega_B$ | $\omega_A$ |
| | $\omega_B - 180$ | $\omega_A$ |
| | $\omega_B$ | $\omega_A - 180$ |
| | $\omega_B - 180$ | $\omega_A - 180$ |
| $\sigma_h$ | $-\omega_A$ | $-\omega_B$ |
| | $180 - \omega_A$ | $-\omega_B$ |
| | $-\omega_A$ | $180 - \omega_B$ |
| | $180 - \omega_A$ | $180 - \omega_B$ |
| $\sigma_v$ | $-\omega_B$ | $-\omega_A$ |
| | $180 - \omega_B$ | $-\omega_A$ |
| | $-\omega_B$ | $180 - \omega_A$ |
| | $180 - \omega_B$ | $180 - \omega_A$ |

$0 \le \omega_A \le 180^\circ$ and $0 \le \omega_B \le 180^\circ$ in seven steps of 30° for each to give a total of 49 individual starting points for optimization. The duplication of points such as $\omega_A = 0^\circ$, $\omega_B = 0^\circ$ and $\omega_A = 180^\circ$, $\omega_B = 180^\circ$ allowed a check on how well this procedure reproduced isometric conformations reached by alternative routes. The resulting structures were found to be within 0.08 kJ mol$^{-1}$ of each other with essentially identical geometries. The 49 individual minimizations were expanded to give a total of 784 points on the potential energy surface through the application of the permutations given in Table 1.†

## 3. Results

### 3.1. *Database study*

The database study retrieved data from 280 different compounds covering a broad spread of transition elements. In these compounds the $PPh_2$ ligand bridges homo- and hetero-bimetallic units both with and without direct metal–metal bonds, as is reflected in the range of $M-M$ distances observed (2.34 to 4.55 Å, see Fig. 1). Perhaps surprisingly there is no correlation of the $M-$P$-M$ and C—P—C bond angles. The mean P—C bond length is 1.832 Å with a sample s.d. of 0.017 Å, [literature value 1.831, sample s.d. 0.016 Å (Orpen *et al.*, 1989)] and the mean C—P—C angle is 101.48° (sample s.d. 2.46°). The softness of the angles is notable (see below). These parameters are correlated, albeit fairly weakly (see Fig. 2); the Spearman rank correlation coefficient (Siegel, 1956) is −0.373, which is significant at the 99% level (see Dunne *et al.*, 1991). A similar correlation of P—C distance and C—P—C angle has been observed in adducts of $PPh_3$ and related species

† Supplementary data for this paper are available from the IUCr electronic archives (Reference: AN0554). Services for accessing these data are described at the back of the journal.

(Dunne *et al.*, 1991; Crispini *et al.*, 1996) and has been interpreted using qualitative molecular orbital methods (Dunne *et al.*, 1991; Gimarc, 1979).

### 3.2. *The potential energy surface of [(AuBr)$_2${$\mu$-PPh$_2$}]$^-$*

The potential energy surface determined for [(AuBr)$_2${$\mu$-PPh$_2$}]$^-$ is shown in Fig. 3. As expected, maxima are observed at $\omega_A \simeq 0^\circ$ and $\omega_B \simeq 0^\circ$ [*i.e.* (0, 0) and positions related by the 180° periodicity of the conformation space] when the two phenyl rings lie coplanar and large non-bonded energies are associated with the *ortho* hydrogen contacts. The potential energy of the maximum at (0, 0) is 116 kJ mol$^{-1}$ with a van der Waals component of 69.5 kJ mol$^{-1}$ and a contribution of 37.3 kJ mol$^{-1}$ from the angle bend term. Surrounding the maxima lie broad low-energy valleys. The global minimum conformation is observed at (60.8, 60.8) and equivalent conformations, the propeller conformation shown in Fig. 4. This is very similar to the conformation of [(AuBr)$_2$PPh$_2$]$^-$ in the crystal structure of its tetrabutylammonium salt (Pritchard *et al.*, 1987), which has $\omega_A = \omega_B = -70.4^\circ$ [equivalent to (70.4, 70.4)]. The total potential energy of the global minimum is 67.0 kJ mol$^{-1}$ with non-bonded and bond energy contributions of 60 and 7 kJ mol$^{-1}$, respectively. The calculated lowest energy structure lies in the broad potential energy well centred around (90, 90), with the contour boundary for the well at 73.7 kJ mol$^{-1}$ (see Fig. 5). Clearly the low steric crowding in [(AuBr)$_2${$\mu$-PPh$_2$}]$^-$ gives rise to large torsions about the P—C(*ipso*) bonds with little variation in the potential energy.

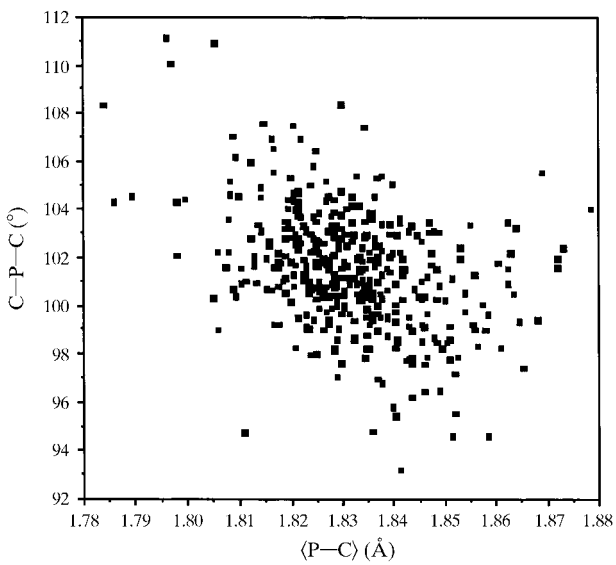


Fig. 2. Scatter plot of average P—C bond lengths (Å) and C—P—C bond angles (°) in the structures from the CSD study of [$M_2${$\mu$-PPh$_2$}].

### 3.3. *Discussion*

A comparison of the geometry of the global minimum conformation with that of [(AuBr)$_2${$\mu$-PPh$_2$}]$^-$ in its crystal structure is given in Table 2. As in other studies using the UFF, the bond lengths are in good to fair agreement with the crystal structure (and with P—C values from the broader CSD study). The bond angles are in fair agreement except the C—P—C angle which is fitted poorly. Both in the crystal structure of [(AuBr)$_2${$\mu$-PPh$_2$}]$^-$ (Pritchard *et al.*, 1987) and in the CSD study presented above, the C—P—C bond angle is substantially smaller than both the UFF calculated value and

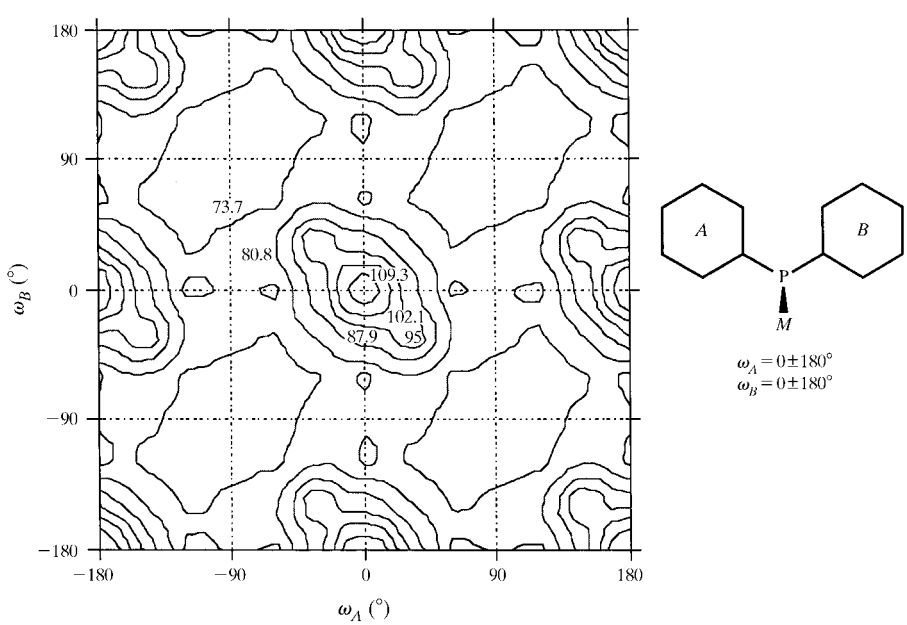


Fig. 3. The potential energy surface for [(AuBr)$_2${$\mu$-PPh$_2$}]$^-$. Energies are given in kJ mol$^{-1}$. Contours are plotted at 7.1 kJ mol$^{-1}$ intervals. The maximum energy conformation (0, 0) is shown.

the ideal tetrahedral value. The UFF natural bond angle at this type of phosphorus is the ideal tetrahedral value (109.5°) and it seems a smaller value (*ca* 101°) would be more appropriate.

In Fig. 5 the results of the CSD database analysis of the conformations of $[M_2\{\mu\text{-PPh}_2\}]$ are projected onto the contour diagram for the $(\omega_A, \omega_B)$ potential energy surface of $[(\text{AuBr})_2\{\mu\text{-PPh}_2\}]^-$. The observed experimental structures fall within the lower-energy regions of the PES, showing good agreement between the calculated relative potential energies of the conformations of $[(\text{AuBr})_2\{\mu\text{-PPh}_2\}]^-$ and the observed conformations of $[M_2\{\mu\text{-PPh}_2\}]$. The scatter plot of the observed $(\omega_A, \omega_B)$ values (Fig. 5) shows large empty regions centred on $\omega_A = 0°$, $\omega_B = 0°$ [*i.e.* (0, 0)] and symmetry-related positions. The $C_{2v}$ symmetry and 180° periodicity of the pattern reflects the frame and rotor symmetry and is as imposed on the PES.

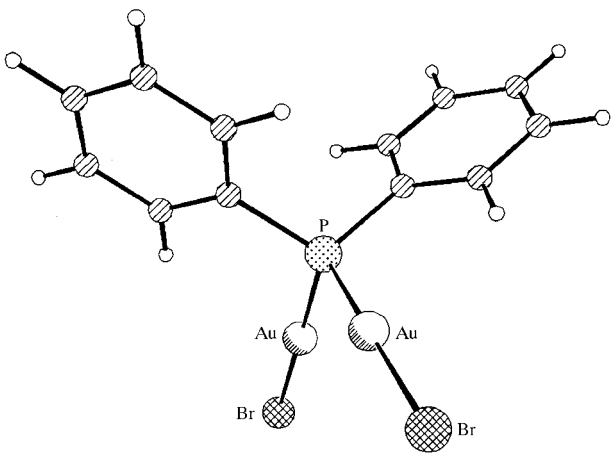


Fig. 4. The global minimum conformation of $[(\text{AuBr})_2\{\mu\text{-PPh}_2\}]^-$.

Table 2. *Comparison of the calculated and experimental (X-ray) structures of* $[(AuBr)_2\{\mu\text{-PPh}_2\}]^-$

Bond lengths are given in Å and angles in °. Experimental s.u.'s are given in parentheses.

| | Calculated | X-ray structure | Δ |
|---|---|---|---|
| Au—Br | 2.420 | 2.401 (2) | 0.02 |
| Au—P | 2.315 | 2.243 (3) | 0.072 |
| P—C | 1.83 | 1.83 (1) | 0.00 |
| Br—Au—P | 179.6 | 176.6 (1) | 3.0 |
| Au—P—Au | 109.6 | 112.1 (2) | 2.5 |
| C—P—C | 109.2 | 102.4 (8) | 6.8 |

The maxima in the PES for $[(\text{AuBr})_2\{\mu\text{-PPh}_2\}]^-$ tend to spread out in the $\omega_A \simeq -\omega_B$ direction, as do the empty regions of the scatter plot for the CSD study of $[M_2\{\mu\text{-PPh}_2\}]$ species. The rotation of the two phenyl rings in opposite directions away from the maximum at (0, 0) maintains the unfavourable non-bonded contacts for longer than the disrotatory motion of the two rings, as shown in Fig. 5. Comparison of the minimized conformer at (30, 30) with that for (30, −30) shows the potential energies to be 80.4 and 105.9 kJ mol$^{-1}$, respectively. It is the bond-angle term which varies most between these two conformations; thus the non-bonded potential energies are 62.8 and 67.8 kJ mol$^{-1}$, respectively, while the angle energy terms are 1.7 and 16.3 kJ mol$^{-1}$. This implies that in cases where non-bonded strain is high the force field alleviates strain by

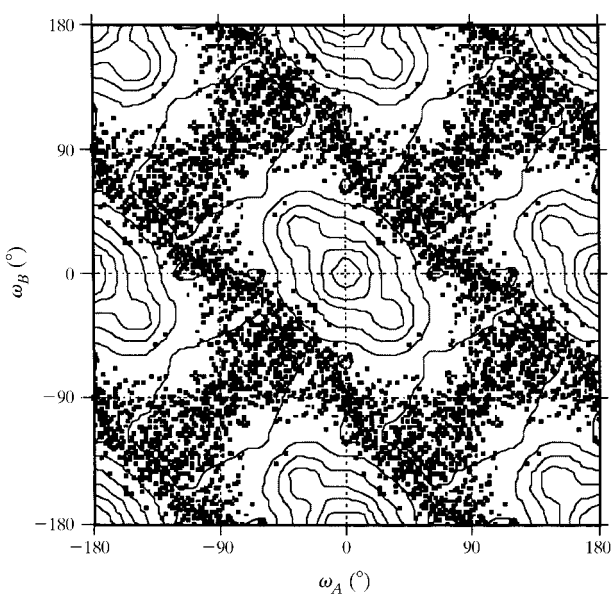


Fig. 5. The distribution of $(\omega_A, \omega_B)$ values (°) for $[M_2\{\mu\text{-PPh}_2\}]$ fragments in crystal structures from the CSD overlaid on the potential energy contour map for $[(\text{AuBr})_2\{\mu\text{-PPh}_2\}]^-$.

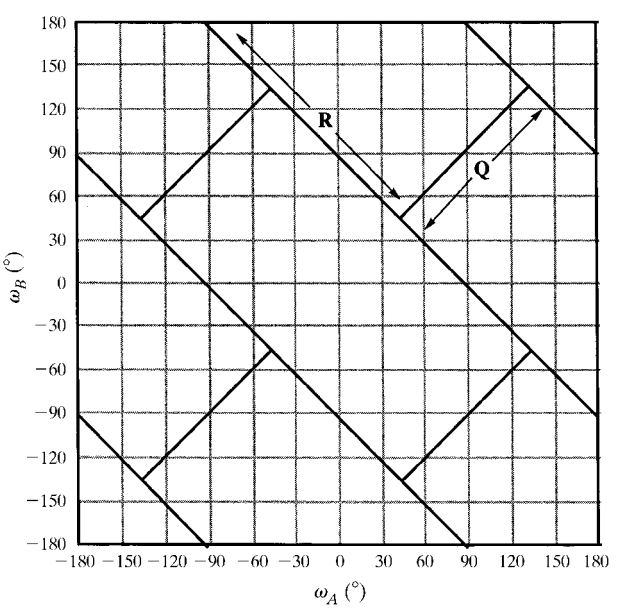


Fig. 6. Idealized low-energy P—Ph rotation pathways through the potential energy surface for $[(\text{AuBr})_2\{\mu\text{-PPh}_2\}]^-$.

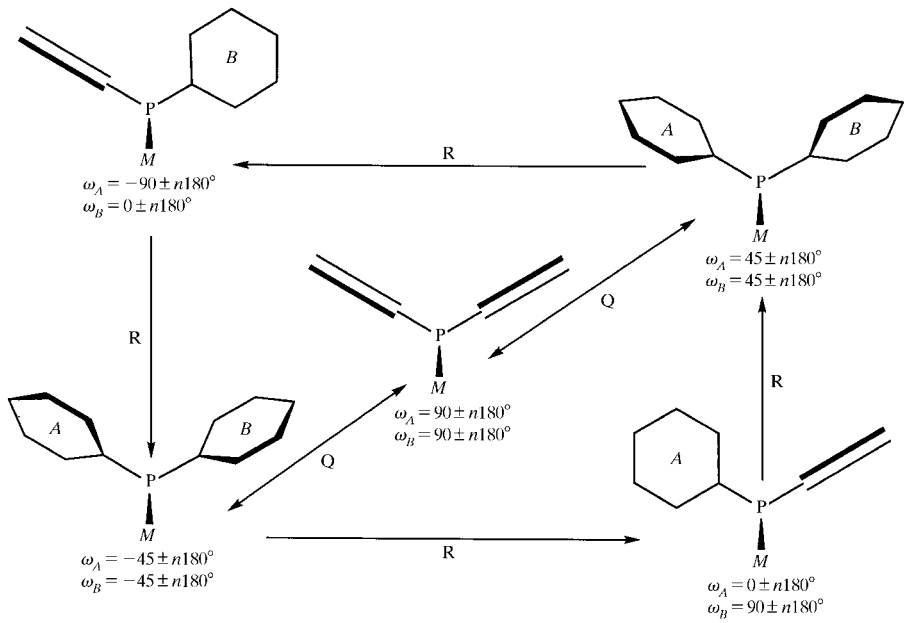


Fig. 7. Mechanisms of phenyl rotation in $[M_2\{\mu\text{-PPh}_2\}]$. Mode **R** for geared phenyl disrotation is shown around the sides of the rectangle, and **Q**, for the conrotation of phenyl rings *A* and *B*, along the diagonal.

the angle deformation rather than through bond stretches. This is consistent with the observed variations in the C—P—C angles noted above in the CSD study.

The positions of the valleys in the PES and the occupied regions of the CSD scatter plot (see Fig. 5) suggest two unique pathways for phenyl rotations, **Q** and **R** (see Fig. 6), which involve only small energy perturbations relative to the global minimum on this energy surface. Mechanism **R** involves geared disrotatory motion of the rings about their P—C(*ipso*) bonds (see Fig. 7). On this pathway the torsion angles obey the relationship $\omega_A + \omega_B = 90 \pm n180°$ and the phenyl rings behave like cogged gears. The second shorter and finite path, **Q**, runs from (45, 45) to (135, 135) along a line of form $\omega_A = \omega_B \pm n180°$. Here the rings do not behave like cogged gears, but rather slip in a conrotatory manner (see Fig. 7) passing through or close to the $C_{2v}$ symmetrical conformation at (90, 90). Phenyl ring rotations in this system therefore occur by progress along **R** or **Q** or a combination of the two. In practice the low-energy regions of the PES are relatively broad and torsion angles may deviate by tens of degrees from these idealized paths without significant energy penalties. Path **R** passes formally through (180, −90), which has a calculated energy of 73.7 kJ mol$^{-1}$, while **Q** passes through the conformer (90, 90) (energy 74.5 kJ mol$^{-1}$). By symmetry this point is at a stationary point of the PES and inspection of the local features of the PES shows it to be a weak maximum. This suggests that the barrier to the slipping mechanism **Q** is *ca* 7.5 kJ mol$^{-1}$, while that for **R**, the geared rotation of the two phenyl rings, is *ca* 6.7 kJ mol$^{-1}$. The difference in these values is at the level of the precision of these energies, as noted above. Both mechanisms are clearly low-energy processes and are likely to occur in solution at ambient temperatures and well below. This is consistent with the full population of these regions as observed in the CSD scatter plot.

There is a clear relationship between this symmetrical system and others for two phenyl rotors attached to a phosphorus atom [such as in *M*(dppe), *M*($\mu$-dppm), $M\text{PPh}_3$ and *M*(tripod) complexes] (see, for example, Morton & Orpen, 1992; Garner & Orpen, 1993; Hunger *et al.*, 1998) previously studied. In all these cases the CSD studies show that the high-energy region around (0, 0) in the notation of this paper is devoid of structures and the populated regions lie within those regions populated in the $[M_2\{\mu\text{-PPh}_2\}]$ system. Other aspects of the local environment in $M\text{PPh}_3$, *M*(dppe), *M*($\mu$-dppm) and *M*(tripod) species lead to partial depopulation of some of the low-energy regions of their equivalent of the ($\omega_A$, $\omega_B$) space as a result of phenyl ring interactions with chelate-ring atoms or other steric factors. In general it seems that all these $\text{PPh}_2$ systems can be viewed satisfactorily as mechanical rotors with a near rigid $\text{PC}_2$ frame and well modelled by molecular mechanics force fields of the quality of the UFF.

We thank the many chemists and crystallographers who synthesized the molecules and determined the structures discussed in this paper.

## References

Allen, F. H. & Kennard, O. (1993). *Chem. Des. Autom. News*, **8**, 31–37.

Baker, R. T., Fultz, W. C., Marder, T. B. & Williams, I. D. (1990). *Organometallics*, **9**, 2357–2367.

Bye, E., Schweizer, W. B. & Dunitz, J. D. (1982). *J. Am. Chem. Soc.* **104**, 5893–5898.

Crispini, A., Harrison, K. N., Orpen, A. G., Pringle, P. G. & Wheatcroft, J. (1996). *J. Chem. Soc. Dalton Trans.* pp. 1069–1076.

Dunitz, J. D. (1979). *X-ray Analysis and the Structure of Organic Molecules*. Ithaca, New York: Cornell University Press.

Dunne, B. J., Morris, R. B. & Orpen, A. G. (1991). *J. Chem. Soc. Dalton Trans.* pp. 653–662.

Garner, S. E. & Orpen, A. G. (1993). *J. Chem. Soc. Dalton Trans.* pp. 533–541.

Gimarc, B. M. (1979). *Molecular Structure and Bonding*. New York: Academic Press.

Hunger, J., Beyreuther, S., Huttner, G., Allinger, K., Radelof, U. & Zsolnai, L. (1998). *Eur. J. Inorg. Chem.* pp. 693–702.

Klebe, G. (1994). *J. Mol. Struct. (Theochem),* **114**, 53–89.

Mislow, K. (1976). *Acc. Chem. Res.* **9**, 26–33.

Molecular Simulations Inc. (1994). *CERIUS*. Version 3.2. Molecular Simulations Inc., The Quorum, Barnwell Road, Cambridge, England.

Morton, D. A. V. & Orpen, A. G. (1992). *J. Chem. Soc. Dalton Trans.* pp. 641–653.

Norskov-Lauritsen, L. & Bürgi, H.-B. (1985). *J. Comput. Chem.* **6**, 216–228.

Orpen, A. G., Brammer, L., Allen, F. H., Kennard, O., Watson, D. G. & Taylor, R. (1989). *J. Chem. Soc. Dalton Trans.* pp. S1–S83.

Pritchard, R. G., Dyson, D. B., Parish, R. V., McAuliffe, C. A. & Beagley, B. (1987). *J. Chem. Soc. Chem. Commun.* pp. 371–372.

Rappé, A. K., Casewit, C. J., Colwell, K. S., Goddard, W. A. III & Skiff, W. M. (1992). *J. Am. Chem. Soc.* **114**, 10024–10034.

Rappoport, Z. & Biali, S. E. (1997). *Acc. Chem. Res.* **30**, 307–314.

Rappoport, Z., Biali, S. E. & Kaftory, M. (1990) *J. Am. Chem. Soc.* **112**, 7742–7748.

Siegel, S. (1956). *Nonparametric Statistics for the Behavioral Sciences*. New York: McGraw-Hill.